Please cite this article as:
Carrasco-Núñez, G., Bernal, J. P., Dávila, P., Jicha, B., Giordano, G., & Hernández, J. (2018). Reappraisal of Los Humeros volcanic complex by new U/Th zircon and 40Ar/39Ar dating: Implications for greater geothermal potential. Geochemistry, Geophysics, Geosystems, 19, 132– 149. DOI: 10.1002/2017GC007044 To view the published open abstract, go to: https://doi.org/10.1002/2017GC007044

AGU PUBLICATIONS

Geochemistry, Geophysics, Geosystems

RESEARCH ARTICLE
10.1002/2017GC007044

Key Points:
- Geochronologic evidence supporting a reappraisal of the evolution of Los Humeros volcanic complex
- Younger ages for Los Humeros volcanic complex imply more favorable conditions for the associated geothermal system
- Modern geochronologic methods redefine duration of the caldera phase (from 410 to 94 kyr)

Supporting Information:
- Supporting Information S1
- Supporting Information S2
- Data Set S1
- Data Set S2

Correspondence to:
G. Carrasco-Núñez,
gerardoc@geociencias.unam.mx

Citation:
Carrasco-Núñez, G., Bernal, J. P., Dávila, P., Jicha, B., Giordano, G., & Hernández, J. (2018). Reappraisal of Los Humeros volcanic complex by new U/Th zircon and $^{40}Ar/^{39}Ar$ dating: Implications for greater geothermal potential. *Geochemistry, Geophysics, Geosystems*, *19*, 132–149. https://doi.org/10.1002/2017GC007044

Received 31 MAY 2017
Accepted 15 DEC 2017
Accepted article online 4 JAN 2018
Published online 19 JAN 2018

Reappraisal of Los Humeros Volcanic Complex by New U/Th Zircon and $^{40}Ar/^{39}Ar$ Dating: Implications for Greater Geothermal Potential

G. Carrasco-Núñez[1], J. P. Bernal[1], P. Dávila[2], B. Jicha[3], G. Giordano[4], and J. Hernández[1]

[1]Campus UNAM Juriquilla, Centro de Geociencias, Universidad Nacional Autónoma de México, Queretaro, Mexico, [2]Instituto Potosino de Investigación Científica y Tecnológica, San Luis Potosí, Mexico, [3]Department of Geoscience, University of Wisconsin-Madison, Madison, WI, USA, [4]Dipartimento di Science, Università Roma Tre, Roma, Italy

Abstract Longevity and size of magmatic systems are fundamental factors for assessing the potential of a geothermal field. At Los Humeros volcanic complex (LHVC), the first caldera-forming event was reported at 460 ± 40 ka. New zircon U/Th and plagioclase $^{40}Ar/^{39}Ar$ dates of pre-, syn- and postcaldera volcanics allow a reappraisal of the evolution of the geothermally active LHVC. The age of the voluminous Xaltipan ignimbrite (115 km^3 dense rock equivalent [DRE]) associated with the formation of the Los Humeros caldera is now constrained by two geochronometers (zircon U/Th and plagioclase $^{40}Ar/^{39}Ar$ dating) to 164 ± 4.2 ka, which postdates a long episode of precaldera volcanism (rhyolitic domes), the oldest age of which is 693.0 ± 1.9 ka ($^{40}Ar/^{39}Ar$). The inferred short residence time (around 5 ka) for the paroxysmal Xaltipan ignimbrite is indicative of rapid assembly of a large magma body and rejuvenation of the system due to recurrent recharge magmas, as it has been occurred in some other large magmatic systems. Younger ages than previously believed have been obtained also for the other voluminous explosive phases of the Faby fall tuff at ~70 ka and the second caldera-forming Zaragoza ignimbrite with 15 km^3 DRE, which erupted immediately after. Thus, the time interval that separates the two caldera-forming episodes at Los Humeros is only 94 kyr, which is a much shorter interval than suggested by previous K-Ar dates (410 kyr). This temporal proximity allows us to propose a caldera stage encompassing the Xaltipan and the Zaragoza ignimbrites, followed by emplacement at 44.8 ± 1.7 ka of rhyolitic magmas interpreted to represent a postcaldera, resurgent stage. Rhyolitic eruptions have also occurred during the Holocene (<7.3 ± 0.1 ka) along with olivine-rich basalts that suggest recharge of the system. The estimated large volume magmatic reservoir for Los Humeros (>~1,200 km^3) and these new ages indicating much younger caldera-forming volcanism than previously believed are fundamental factors in the application of classical conductive models of heat resource, enhancing the heat production capacity and favor a higher geothermal potential.

Plain Language Summary More recent ages obtained for Los Humeros volcano may increase the heat capacity of the magmatic chamber at depth, providing more favorable conditions for the development of the geothermal energy.

1. Introduction

Silicic caldera-forming systems involve the rapid evacuation and sudden decompression of voluminous magmatic reservoirs, giving rise to large collapse calderas, several kilometers in diameter (i.e., Branney, 1995; Cole et al., 2005; Druitt & Sparks, 1984; Lipman, 1997; Martí, 1991; Scandone, 1990). Large calderas have been traditionally associated with relatively shallow, long-lived crustal magma chambers (i.e., Brown & Fletcher 1999; Reid & Coath 2000; Reid et al., 1997). However, recent studies of large silicic systems call upon complex and heterogeneous magma reservoirs and processes (e.g., Cashman & Giordano, 2014; Cashman et al., 2017; Gualda & Ghiorso, 2013; Hildreth & Wilson, 2007; Hildreth, 2004; Lipman, 2007), including tapping multiple melt lenses stored within a largely crystalline mush (Bachmann & Bergantz, 2004; Cooper et al., 2012; Ellis et al., 2010; Wotzlaw et al., 2014), variable magma accumulation from short lived (e.g., Mathews et al., 2015; Rivera et al., 2014) to prolonged melt extraction (up to 100–150 kyr; Deering et al., 2016; Wotzlaw et al., 2013), and magma replenishment and mixing with residual phases of older silicic magma chambers. Caldera subsidence after the withdrawal of a critical volume of magma can be

related to the depth and geometry of the reservoir (e.g., Geshi et al., 2014; Geyer et al., 2006; Roche & Druitt, 2001).

The longevity of magmatic systems is important to the development of mature geothermal systems, providing heat for hundreds of thousands of years or even up to several millions of years (e.g., Taupo Volcanic Zone [Wilson et al., 2009]; Long Valley [Reid & Coath, 2000; Reid et al., 1997]). However, available data show that there is not a good correlation between magma volume and residence times for large volume caldera-forming eruptions (>100 km^3), as they range from some kyr to a few 100s kyr (Costa, 2008). Volcanic systems that have developed calderas commonly host long-lived hydrothermal systems and these can form important geothermal resources. The complexity of these volcanic structures, such as the case of Los Humeros Volcanic Complex (LHVC) in Mexico, may involve repetitive caldera collapse events, alternating episodes of effusive and explosive events, central and ring-fracture effusions of lava flows and/or intrusions of domes in late stages as a resurgence postcaldera stage (e.g., the Central Italy Geothermal Province; Giordano et al., 2014).

Extensive fieldwork for over a decade, supported with new zircon-U/Th and $^{40}Ar/^{39}Ar$ dates, provide support for a new evolutionary scheme of the LHVC with important implications on the thermal fingerprint of the magmatic heat source in the geothermal system. Our results indicate a much younger age for the caldera-forming event (164 ± 4.2 ka), less than half of the previously reported age of 460 ka (Ferriz & Mahood, 1984). Given that the volume of the major caldera-forming ignimbrite (Xaltipan) is at least 115 km^3, this younger age is particularly important because it implies that the associated geothermal system is related to a very young heat source. Thus, the geothermal potential must be reassessed.

1.1. Geological Setting

The LHVC is the largest active caldera of the Trans-Mexican Volcanic Belt (TMVB), comprising a geothermal field currently in exploitation producing about 65 MW power. It is a Pleistocene-Holocene, basaltic andesite-rhyolite caldera system (Ferriz & Mahood, 1984, 1987; Yáñez & García, 1982), located in the northern part of the eastern TMVB (Figure 1). It is located in the Serdán-Oriental Basin, which is characterized by Quaternary monogenetic bimodal volcanism with cinder cones, basaltic and rhyolitic maars, and rhyolitic domes. The regional basement is formed by the Teziutlán Massif comprising a Paleozoic-Mesozoic crystalline complex, made of metamorphic and intrusive rocks, including green schists, granodiorites, and granites (246–131 Ma, K/Ar; Yáñez & García, 1982). This basement is partially covered by a thick, highly deformed Mesozoic sedimentary succession that belongs to the Sierra Madre Oriental fold and thrust province. Oligocene to Miocene granodiorite and syenite intrusions are also exposed within the area (31–15 Ma; Yáñez & García, 1982). Slightly younger, Miocene (11–9 Ma, K/Ar; Carrasco-Núñez et al., 1997; Gómez-Tuena & Carrasco-Núñez, 2000) and Pliocene-lower Pleistocene andesitic volcanism (Ferriz & Mahood, 1984; Yáñez & García, 1982) is present to the north of the caldera, and represents the thick, andesitic successions forming the subsurface geology of Los Humeros volcano (2.61–1.46 Ma; Carrasco-Núñez et al., 2017b).

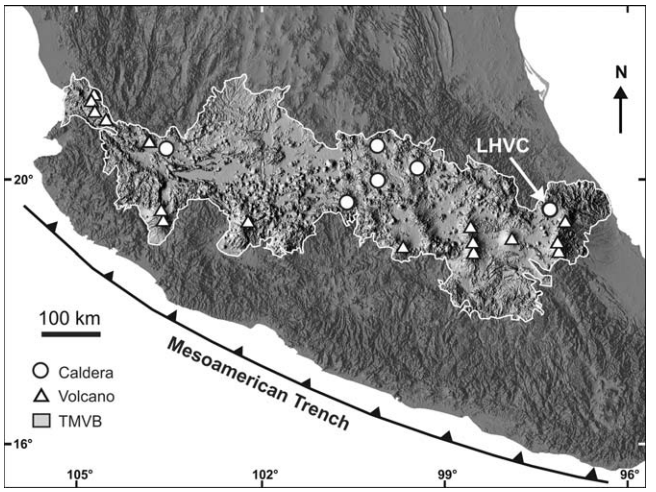

Figure 1. Location of LHVC and geothermal field in the eastern sector of TMVB.

First attempts to define the geology and stratigraphy of LHVC were made in the late 1970s and early 1980s (De la Cruz, 1983; Perez-Reynoso, 1978; Yáñez & García, 1982) until a more comprehensive description of its volcanological evolution was proposed by Ferriz and Mahood (1984). A compiled geological map of the volcanic area was recently obtained (Carrasco-Núñez et al., 2017b) and an updated version is now available (Carrasco-Núñez et al., 2017a). A simplified version of this map is presented in Figure 2.

1.2. Previous Data on the Stratigraphy of LHVC

Ferriz and Mahood (1984), based on stratigraphy and K/Ar data, proposed a reconstruction of the volcanic evolution of LHVC, which until today has been taken as the basis for all subsequent studies. We hereafter summarize their geochronologic data and volcanological interpretations. Following the eruption of isolated high-silica rhyolite lavas dated at 470 ± 80 ka (sanidine) (note that both published and new

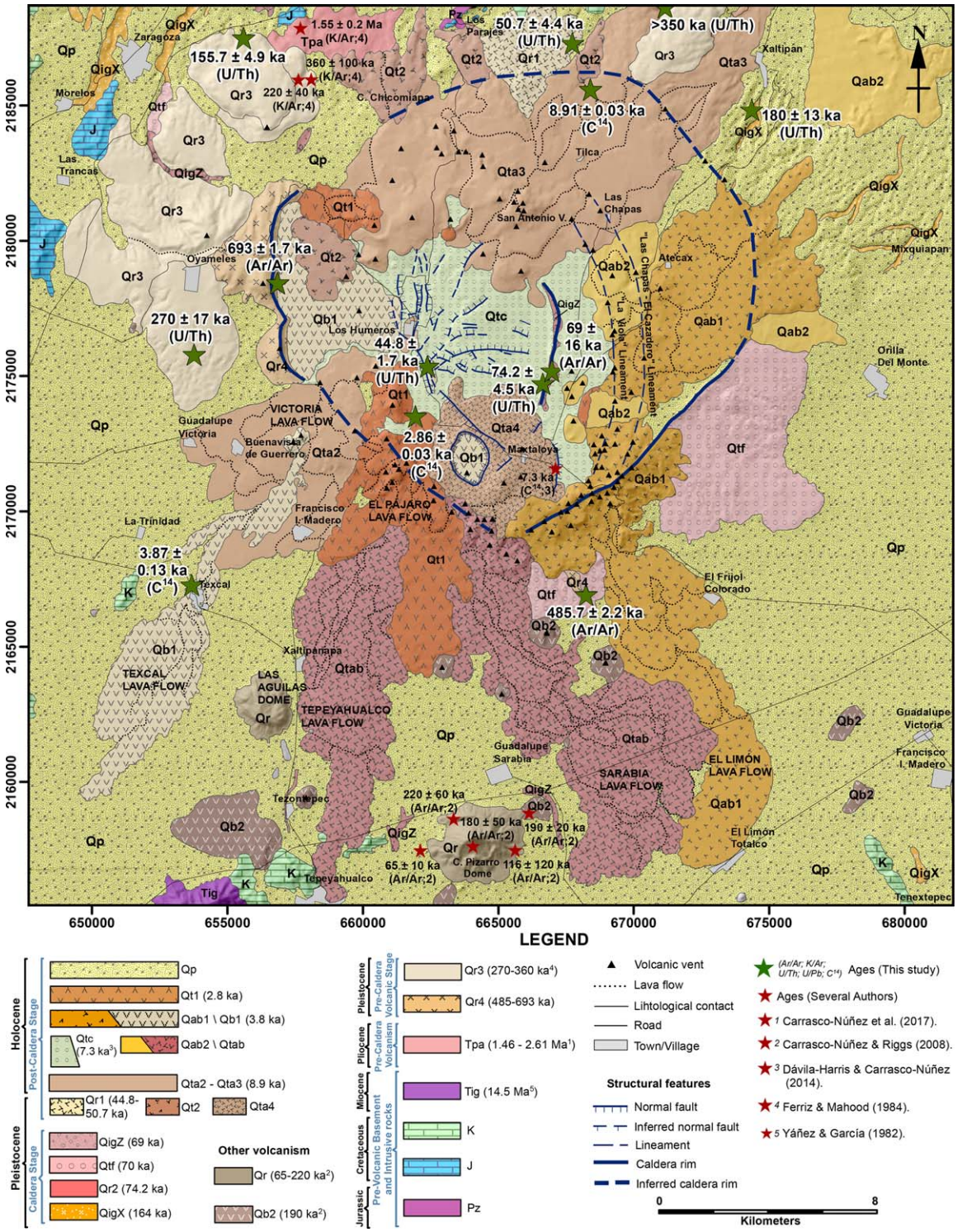

Figure 2. Simplified geologic map of Los Humeros caldera and geothermal field. A larger-scale map with a full description of each of these lithostratigraphic units can be found in Carrasco-Núñez et al. (2017a). Key for the lithological rock units: Prevolcanic basement—Pz/K, granodiorites and schists; J, limestones and shales; K, limestones; Tig, granite; precaldera volcanism—Tpa, Teziutlán basaltic lavas; precaldera-volcanic stage—Qr4, rhyolitic domes; Qr3, rhyolitic domes; Other volcanism—Qb2, basalts and basaltic andesites; Qr, C. Pizarro-Águilas rhyolitic domes; caldera stage—QigX, Xaltipan ignimbrite; Qr2, Los Potreros rhyolitic dikes; Qtf, Faby Tuff; QigZ, Zaragoza ignimbrite; postcaldera stage—resurgent phase: Qt2, Chicomiapa-Los Parajes trahyites; Qr1, rhyolitic domes; Qta4, Maxtaloya trachyandesites; ring-fracture and bimodal phase: Qta2, Victoria trachyandesites; Qtab, Tepeyahualco basaltic trachyandesites; Qab1, Atecax basaltic andesites; Qab2, basaltic andesites; Qta3, San Antonio-Las Chapas trachyandesites; Qtc, Cuicuiltic member; Qb1, olivine basaltic lavas; Qt1, El Pájaro trachytes; Qp, undetermined pyroclastic deposits.

data hereafter are reported with 2σ), the first caldera-forming eruption occurred with the emplacement of the voluminous and paroxysmal Xaltipan ignimbrite (~115 km^3 DRE) and formation of an irregular-shaped 21 × 15 km wide caldera (Los Humeros) with an area of 260 km^2. The ignimbrite was dated by K/Ar at 460 ± 260 (biotite) and 460 ± 40 ka (plagioclase). After the caldera collapse, alternating explosive and effusive activity including the emplacement of high-silica rhyolite domes dated at 360 ± 100 ka (sanidine) to 220 ± 40 ka (sanidine) (Ferriz & Mahood, 1984), and was followed by a succession of repetitive rhyodacitic Plinian pumice fallout deposits, named the Faby Tuff, totaling ~10 km^3 (DRE). K-Ar dates for the Faby Tuff range from 270 ± 60 ka (plagioclase) to 190 ± 80 ka (plagioclase) (Ferriz & Mahood, 1984). Willcox (2011) provided slightly younger $^{40}Ar/^{39}Ar$ ages for the Faby Tuff, ranging from 140 ± 40 to 260 ± 80 ka (plagioclase).

A second caldera-forming episode was identified, forming the 9 km × 10 km Los Potreros caldera nested inside the larger Los Humeros caldera (Figure 2). The Los Potreros caldera is associated with the emplacement of the 15 km^3 Zaragoza ignimbrite (Carrasco-Núñez et al., 2015) dated by Willcox (2011) at 140 ± 24 ka (plagioclase). This was followed by the emplacement of rhyodacitic lavas K-Ar dated (Ferriz & Mahood, 1984) at 60 ± 20 ka (glass). The activity reconstructed by Ferriz and Mahood (1984) continued with explosive eruptions, producing dacitic pumice fall units (Xoxoctic Tuff, 0.6 km^3 at ~50 ka) and pyroclastic flows and breccia deposits (Llano Tuff) and the formation of the 1.7 km diameter Xalapazco crater. Subsequent andesitic and basaltic andesite lavas erupted through ring-fractures into the northern and southern sectors of Los Humeros caldera, and those to the northern area in the caldera interior were dated at 40 ± 60 (whole rock), 30 ± 40 (whole rock), 20 ± 60 (whole rock), and 20 ± 20 (whole rock) ka (Ferriz & Mahood, 1984). Holocene explosive activity has occurred in the caldera's interior with the eruption of about 1 km^3 of rhyodacitic and andesitic tephra.

2. U/Th and $^{40}Ar/^{39}Ar$ Methods and Results

2.1. Zircon U/Th Dating

Age determinations on seven rock samples from different lithostratigraphic units were obtained from $^{230}Th/U$ on zircon grains by LA-MC-ICPMS at Laboratorio de Estudios Isotópicos, Centro de Geociencias, Campus UNAM-Juriquilla, Queretaro, Mexico. The system is comprised of a Resonetics L-50 laser-ablation workstation previously described (Müller et al., 2009; Solari et al., 2010), coupled with a Thermo Finnigan Neptune-Plus MC-ICPMS following the methodology of Bernal et al. (2014). Zircon grains were separated using standard heavy-mineral extraction techniques and mounted in epoxy resin, polished, and screened for potential complex overgrowths by cathodoluminescence. Data analyses and reduction was done using Iolite (Paton et al., 2011) and a custom-made script for these analyses that automatically performs background corrections, mass-bias correction, and isotope and activity ratio calculation. Activity ratios and ages were calculated using the ^{230}Th, ^{232}Th, and ^{238}U half-lives from Audi et al. (1997), Cheng et al. (2013), and Jaffey et al. (1971), respectively. Precision and accuracy was continuously assessed by analyzing two zircon samples known to be at secular equilibrium: standard zircon 91500 with a U/Pb age = 1,065 ± 0.6 Ma (Wiedenbeck et al., 2004), and our lab internal standard, Panchita zircon, with a U/Pb age = 959 ± 1.4 Ma (Solari et al., 2015). Results from more than 450 independent analyses for each zircon obtained during 30 different analytical sessions attest for the high reproducibility and precision of the methodology used here, with $(^{230}Th/^{238}U) = 1.0004 \pm 0.0019$ (2xSE, n = 506, MSWD = 1.06) for 91500 zircon and $(^{230}Th/^{238}U) = 1.0015 \pm 0.0018$ (2xSE, n = 460, MSWD = 1.08) for Panchita zircon. We note that all ratios between brackets denote activity ratios.

When applicable, isochrons and age-calculations were done using Isoplot 3.75 (Ludwig, 2012) following the U-Th systematics detailed in Schmitt (2011). However, for those samples whose $(^{238}U/^{232}Th)$-$(^{230}Th/^{232}Th)$ composition of the zircons revealed a complex crystallization history (i.e., not forming an isochron), suggesting a nonsteady state magma chamber (e.g., Barboni et al., 2016). Alternatively, it can be considered a protracted crystallization from a compositionally heterogeneous magma reservoir where two magmas (rhyodacite and andesitic) apparently remained isolated from one another, possibly as separated interconnected lenses, which interacted in that isotopically homogeneous, but variably crystalized magmatic reservoir as deducted from the Zaragoza ignimbrite (Carrasco-Núñez et al., 2012). U-Th model-ages for each zircon grain were calculated following the "BBB" model (Boehnke et al., 2016). For these samples, the age of

was estimated using the youngest-detrital-zircon algorithm from Isoplot 3.76 (Ludwig, 2012), or by calculating an error-weighted average from a normally distributed U-Th age population. All uncertainties were quadratically expanded at the 2 sigma level.

U/Th zircon ages for the Xaltipan ignimbrite reveal that the selected samples do not represent the same history of crystallization and magma residence, as some samples form isochrons with an age that is coincident with the eruptive age, while others record a more protracted crystallization history and contain antecrysts/xenocrysts (e.g., they do not form an isochron and/or lie on the equiline) (Figure 3). Some of these xenocrysts can be incorporated prior to large eruptions (e.g., Gardner et al., 2002). Regardless of this, all samples have U-Th ages that range between 158 ± 8.3 and 180 + 13 – 12 kyr. These are in excellent agreement with those recently reported also for the Xaltipan ignimbrite from Zapotitlán, Puebla, 166^{+12}_{-11} ka, and Las Minas, Puebla, $168^{+7.7}_{-7.5}$ ka (Aliaga-Campuzano et al., 2017), and $^{40}Ar/^{39}Ar$ age of 157 ± 20.4 ka for plagioclase also from the Xaltipan ignimbrite (Willcox, 2011). All these dates combined yield an emplacement age for the Xaltipan ignimbrite of 164.0 ± 4.2 ka (MSWD 2.1, p = 0.05), as they are statistically identical (Figure 3f). This age is significantly younger than the K-Ar ages reported by Ferriz and Mahood (1984) from biotite (460 ± 260 ka) and plagioclase (460 ± 40 ka) concentrates extracted from the Xaltipan ignimbrite.

We also obtained U-Th zircon ages from several precaldera and postcaldera rhyolitic domes and dikes, but, unfortunately, we were unable to extract zircon grains from the Zaragoza and Faby Tuffs. From the analyzed samples, HK-1408 (dome), HK-1410 (dike), HK-1443 (dome), and HK-14–21 (dome) yield geochronological meaningful isochrons (i.e., statistically robust sense Ludwig and Titterington, 1994) in the ($^{230}Th/^{232}Th$) versus ($^{238}U/^{232}Th$) space, with U-Th ages of 44.8 ± 1.7, $74.2^{+4.4}_{-4.5}$, $155.7^{+4.6}_{-4.9}$, and 270^{+17}_{-15} ka, respectively (Figure 4). Zircon grains from other samples also yielded isochrons that were indistinguishable from the 1:1 equiline, and are thus considered to be in secular equilibrium, with a U-Th age > 350 ka (supporting information SI).

2.2. Plagioclase $^{40}Ar/^{39}Ar$ Dating

Even though Los Humeros lavas and the ignimbrites exhibit slight alteration and minor oxidation, fresh plagioclase crystals were isolated from all units for $^{40}Ar/^{39}Ar$ dating. All samples were irradiated in the CLICIT facility at the Oregon State University TRIGA reactor for 3 h. The Alder Creek rhyolite sanidine was used as a neutron fluence monitor. Several recent experiments have obtained undistinguishable age data for the Alder Creek sanidine standard (Jicha et al., 2016; Niespolo et al., 2017; Rivera et al., 2013). All ages in this study are reported with 2σ analytical uncertainties and are calculated relative to 1.1864 ± 0.0012 Ma (Jicha et al., 2016) using the decay constant of Min et al. (2000).

For the ignimbrites and fall deposits, single crystal fusion experiments were performed, whereas ~20 mg of plagioclase from the precaldera lavas was incrementally heated in 24–25 steps (supporting information SII). All experiments were conducted using a 60W CO_2 laser, and the gas released from the samples was analyzed using a Noblesse multicollector mass spectrometer following the procedures outlined in Jicha et al. (2016).

Two precaldera lavas were dated 486.5 ± 2.4 and 693.0 ± 1.9 ka (Figure 5 and Table 1). Single crystal fusion of feldspar from the Xaltipan ignimbrite gives a weighted mean age of 153 ± 13 ka (n = 15 of 20; MSWD = 0.91). Ages for other important explosive units include the recurrent Plinian succession (Faby fall tuff) at 70 ± 23 ka (n = 17 of 22; MSWD = 0.52) and the second caldera-forming Zaragoza ignimbrite with 15 km^3 at 69 ± 16 ka (n = 16 of 24; MSWD = 0.58) (Figure 5). Episodic resurgent rhyolitic domes, one of which was dated at 50.7 ± 4.4 ka, erupted from 45 to 74 ka (U/Th, this paper), just before and after the Zaragoza ignimbrite.

The large age uncertainty for these young explosive units is due to the relative low K content (K/Ca = 0.06–0.16) of the plagioclase analyzed for single crystal fusion measurements. Owing to rapid diffusion of Ar at magmatic temperatures, $^{40}Ar/^{39}Ar$ dates are commonly interpreted as eruption ages without the ambiguity of protracted crystallization intervals recorded by U-Pb dates of accessory phases. However, dispersion of the nominal dates produced by plagioclase fusion analysis, such as those observed in this study, is becoming more common and is typically attributed to partially degassed antecrysts or xenocrysts or excess Ar (Ellis et al., 2017).

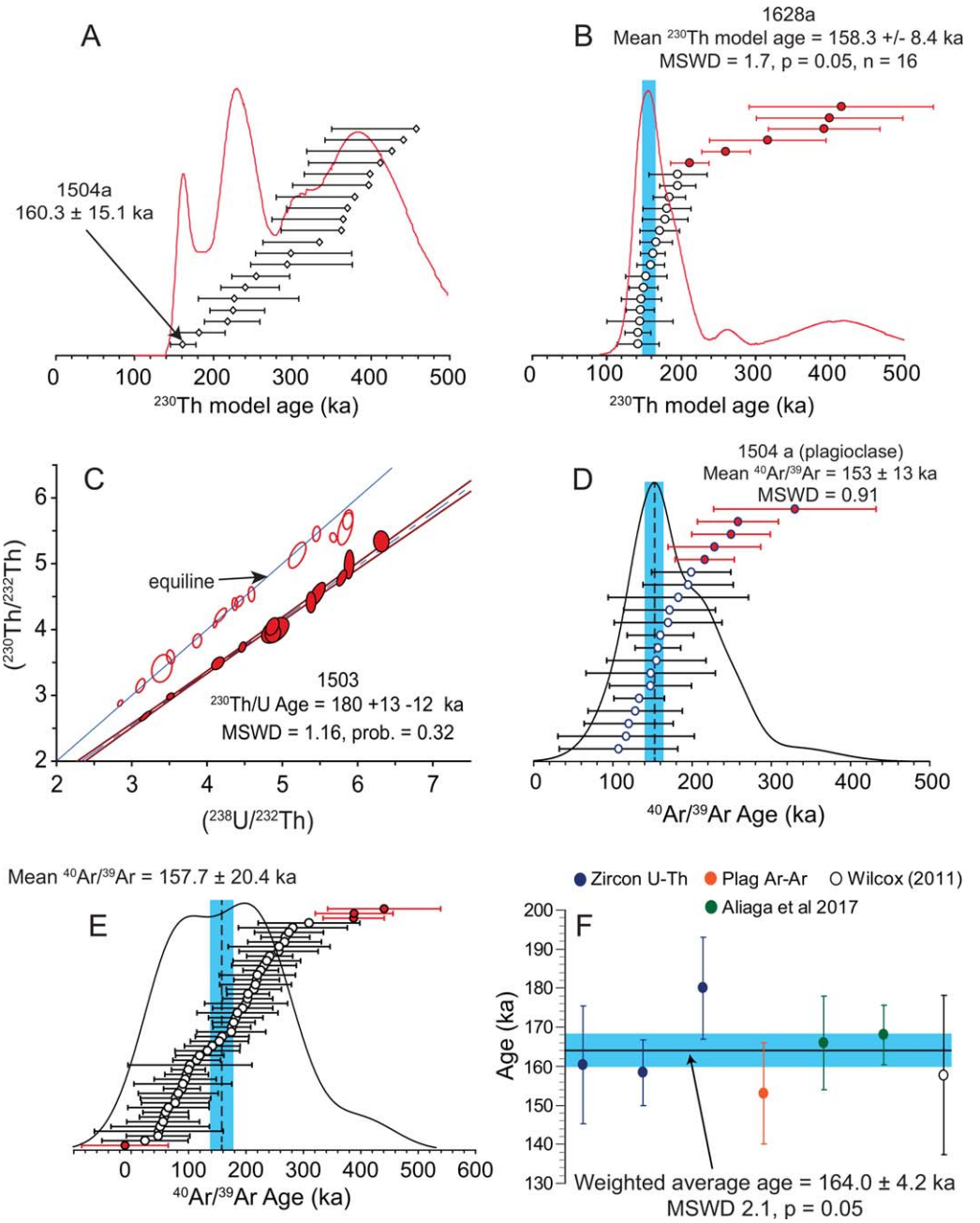

Figure 3. U-Th zircon ages for different samples from the Xaltipan ignimbrite indicating a significantly younger age from the 0.46 Ma initially obtained by Ferriz and Mahood (1984) by K-Ar. (a) ^{230}Th model ages for sample 1504a from the eastern sector of the caldera, the age distribution suggests protracted crystallization from a heterogeneous magma chamber, the age is calculated from the zircon-grain with the youngest ^{230}Th model age. Note that for older samples it was not possible to calculate the upper level uncertainty as it is beyond secular equilibrium. (b) ^{230}Th model ages for sample 1628a from the western sector of the caldera; the age distribution indicates that most zircons crystallized $158.4^{+8.}_{-8.}$ ka (MSWD = 1.7, p 0.05, n = 16). Data in red were not considered in weighted average calculation. (c) Isochron for sample 1503 from the Xaltipan-type section, showing two distinct age-populations; one forming an isochron that yields a U-Th age of 180^{+13}_{-12}ka, and a second plotting upon the equiline. (d) Rank order plot of new ^{40}Ar/^{39}Ar single crystal (plagioclase) fusion data from the Xaltipan ignimbrite. Each data point shown with 2σ analytical uncertainties. Data in red were not considered for age calculations. (e) Rank order plot of ^{40}Ar/^{39}Ar multicrystal (plagioclase) fusion data from the Xaltipan ignimbrite from Willcox (2011). Each data point shown with 2σ analytical uncertainties. (F) summary of U-Th and Ar-Ar ages obtained and previously published for the Xaltipan ignimbrite yielding a weighted average age of 164 $\pm$ 4.2 ka.

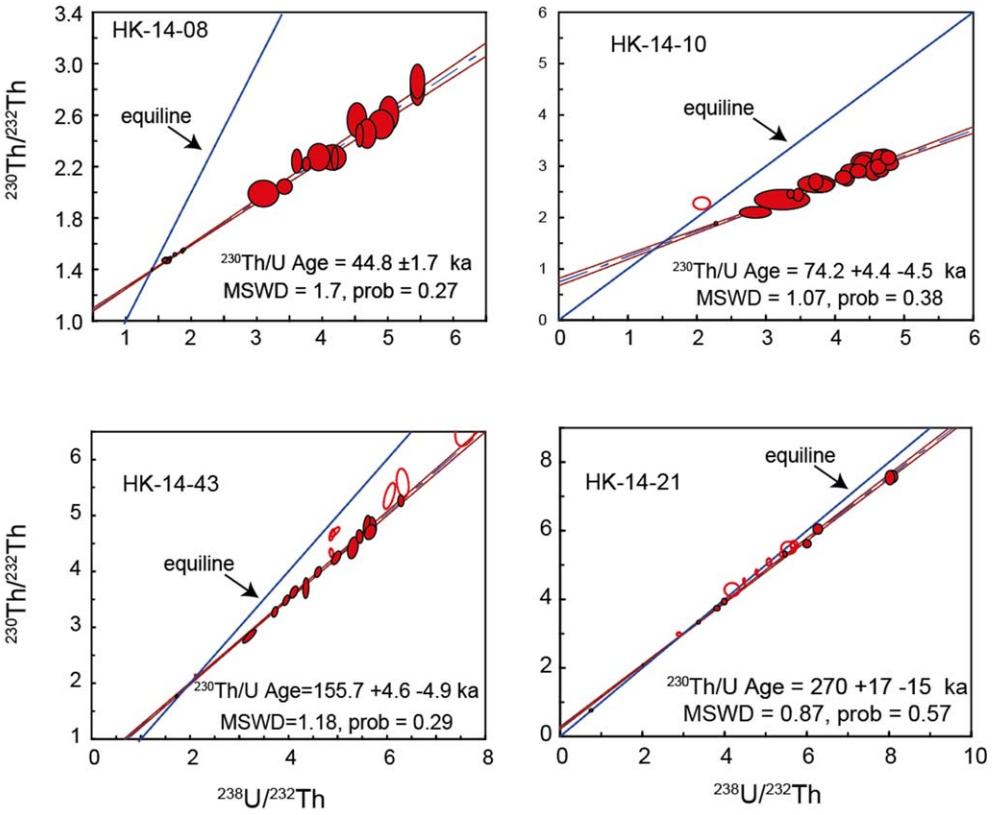

Figure 4. ($^{238}U/^{232}Th$) versus ($^{230}Th/^{232}Th$) Isochrons for domes and rhyolitic lavas postdating the emplacement of the Xaltipan ignimbrite. Open ovals not used to calculate the isochron. All uncertainties expressed at 2 sigma level.

The large discrepancy between the 30+ year old K-Ar data and the new $^{40}Ar/^{39}Ar$ and U-Th data are likely due to the fact that the amount of material required for the K-Ar analyses was several grams versus single crystal analyses performed in this study. There are many documented instances of K-Ar ages being too old when compared to newer generation Ar/Ar ages (e.g., Heizler et al., 1999). Incorporation of xenocrysts or antecrysts into the large bulk separate required for the K-Ar analyses may have resulted in K-Ar ages older than the apparent eruption ages, although in some cases may be due to crystals retaining some mantle or inherited ^{40}Ar (Bachmann et al., 2010; Ellis et al., 2017). Moreover, a similar age of 164 ± 4.2 ka for the Xaltipan ignimbrite was obtained by two independent geochronometers (Table 2), which suggests that the new data in this study is likely more accurate.

3. Discussion

3.1. Reappraisal of the Onset and Recent Evolution of LHVC

With the new ages presented herein, we can define a rather different behavior of the magmatic system at Los Humeros, than previously recognized. For example, the duration of the caldera stage was previously believed to have lasted ~410 kyr (Figure 6), from the first caldera-forming Xaltipan eruption to the youngest caldera-forming Zaragoza eruption. This time frame has now been reduced to approximately 85 kyr. This is especially important because it increases the frequency of large-volume explosive eruptions.

To ease the description of the volcanic evolution of LHVC, the volcanic stratigraphy has been subdivided into three main stages, based on age and type of eruption activity: (1) *precaldera stage*; (2) *caldera stage*, and (3) *postcaldera stage* (Figure 8). The caldera stage includes three phases: (a) *caldera-forming phase 1*, (b) *Plinian phase*, and (c) *caldera-forming phase 2*. The postcaldera stage includes: (a) *resurgence phase* and (b) *ring-fracture and bimodal phase*. A summary of the age determinations presented in this paper and the resulting stratigraphic scheme is shown in Figure 8, which is compared with previous works (Figure 6).

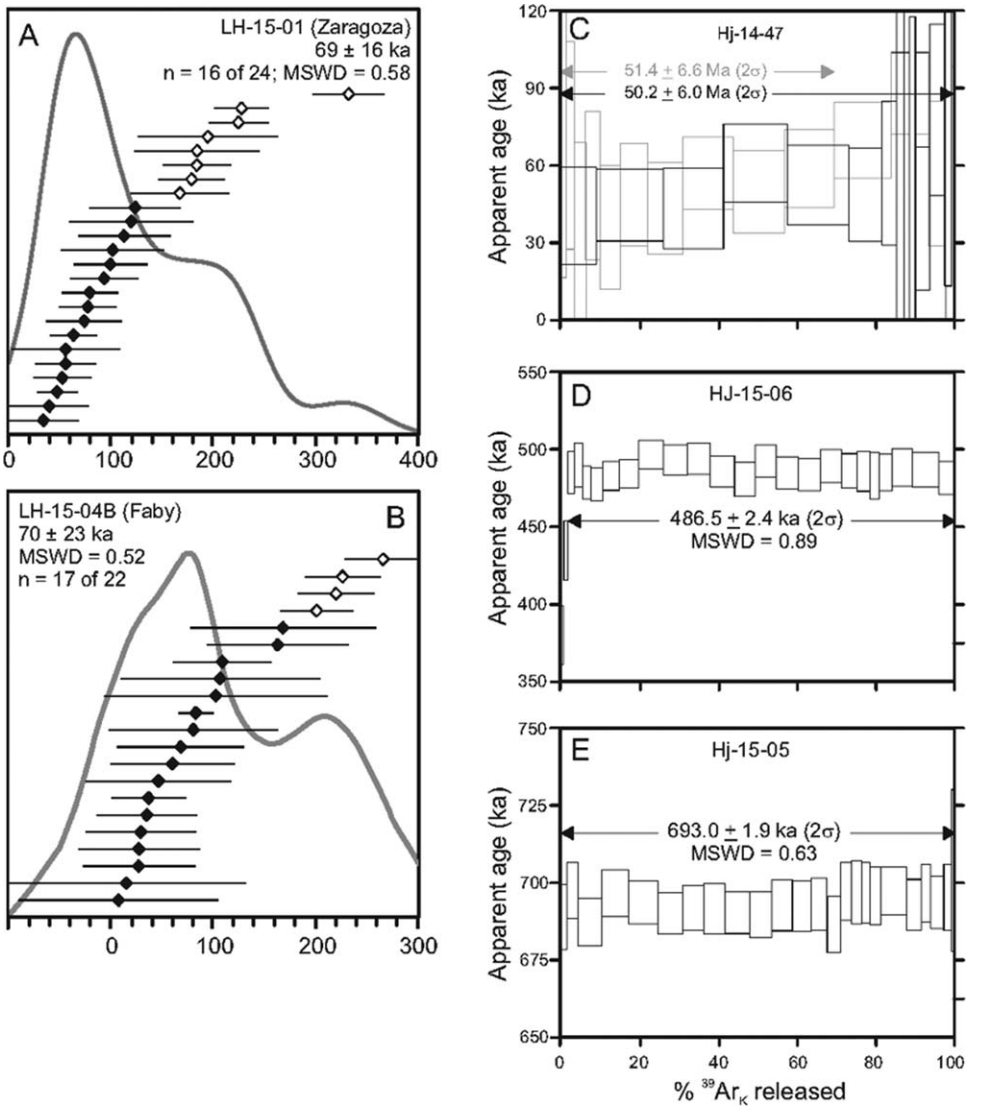

Figure 5. Rank order plots with probability density curves for the single crystal fusions data sets from the (a) Zaragoza ignimbrite and (b) Faby Tuff/Plinian fallout deposits. Data are shown with 1σ analytical uncertainties, whereas weighted mean ages are shown with 2σ analytical uncertainties. Dates with open symbols are excluded from weighted mean calculations. One date is >350 ka, and is not shown. (c, d) Age spectrum diagrams for two precaldera and one postcaldera rhyolite. Plateau steps and ages are shown with 2σ analytical uncertainties. (e) Recalculated age from Willcox (2011).

3.1.1. Precaldera Stage

This stage includes both partially buried rhyolitic lavas and relatively abundant rhyolitic domes erupted to the western side of Los Humeros caldera. This first group comprises two sites: an isolated spot to the south of the caldera reported in this paper at 486.5 ± 2.4 ($^{40}Ar/^{39}Ar$; see Figure 6), which was already dated at 470 ± 80 ka ($^{40}Ar/^{39}Ar$; see Figure 6) by Ferriz and Mahood (1984). The second site is a vitrophyric rhyolite dome truncated by the western scarp, which we report here at 693.0 ± 1.9 ka ($^{40}Ar/^{39}Ar$; see Figure 6). We report a date of 270 ± 17 ka (U/Th, zircon) for a rhyolitic dome that is within the range of other domes of the western sector outside the caldera (see Figure 2) that were previously K-Ar dated at 360 ± 100 and 220 ± 40 ka (Ferriz & Mahood, 1984). Contrary to previous interpretations based on the older ages provided by K-Ar dating of the Xaltipan ignimbrite, these outer rhyolitic domes represent now precaldera volcanism as they are older than the first caldera-forming event (Los Humeros collapse). We remark here that field evidence of dissection of some domes across the caldera margin is in agreement with their new stratigraphic position as precaldera.

Table 1
Summary of $^{40}Ar/^{39}Ar$ Experiments[a]

Sample #	K/Ca total	Total fusion age (ka) ± 2σ	$^{40}Ar/^{36}Ar_i$ ± 2σ	Isochron age (ka) ± 2σ	N	^{39}Ar %	MSWD	Plateau age (ka) ± 2σ
Incremental heating experiments								
HJ-15-06	3.05	485.7 ± 2.2	296.6 ± 5.9	488.3 ± 2.9	23 of 25	98.1	0.89	486.5 ± 2.4
HJ-15-05	20.42	693.0 ± 1.7	294.2 ± 5.4	694.4 ± 2.0	24 of 24	100	0.63	693.0 ± 1.9
HJ-14–47	0.27	57.3 ± 5.4	297 ± 11	60 ± 140	10 of 14	69.4	0.77	51.4 ± 6.6
HJ-14–47	0.25	51.9 ± 5.7	300 ± 11	47 ± 88	13 of 14	99.2	0.84	50.2 ± 6.0
Weighted mean plateau and isochron ages				51 ± 73	23 of 28			50.7 ± 4.4
					N		MSWD	Weighted mean Age (ka) ± 2σ
Single crystal fusion experiments								
LH-15-01	0.16	Plagioclase			16 of 24		0.58	69 ± 16
LH-15-04B	0.06	Plagioclase			17 of 22		0.52	70 ± 23
LH-15-04a	0.40	Plagioclase			15 of 20		0.91	153 ± 13

[a]Ages calculated relative to the 1.1864 Ma Alder Creek sanidine (Jicha et al., 2016; Rivera et al., 2013).

3.2. Caldera Stage

3.2.1. Caldera-Forming Phase 1 (Xaltipan)

The largest of the caldera-forming eruptions of Los Humeros is associated with the emplacement of the Xaltipan ignimbrite (~115 km^3: DRE; Figures 2 and 7a). This event was previously dated at ~460 kyr (Ferriz & Mahood, 1984); however, in this work, the age is revised to 164.0 ± 4.2 ka based on U-Th dating of zircons and $^{40}Ar/^{39}Ar$ dating of plagioclase (Figure 3). Our proposed age of the Xaltipan ignimbrite is in agreement with Willcox (2011), who reported an age of 170 ± 50 ka (plagioclase), but recalculated in this paper as 157.7± 20.4 ka (see Figure 3e), for a pyroclastic flow deposit that directly overlies precaldera andesites, and that we believe corresponds stratigraphically to the Xaltipan ignimbrite. A rhyolitic dome emplaced outside of Los Humeros caldera shows a date of 155.7 ± 4.9 (U/Th, zircon), indicating that extra-caldera rhyolitic volcanism occurred not only during the precaldera stage but also after the main caldera collapse.

3.2.2. Plinian Phase (Faby)

After the Los Humeros caldera collapse, activity was initially dominated by a sequence of several rhyodacitic pumice fallout layers separated by various paleosoils (Figure 7b), which are collectively grouped as the Faby Tuff (Ferriz & Mahood, 1984; Willcox, 2011). Our data indicate an $^{40}Ar/^{39}Ar$ date of 70 ± 23 ka for the lowermost member.

Table 2
Summary of the U/Th and Ar/Ar Dates for Los Humeros Caldera and Geothermal Field

				U-Th dating		Ar-Ar dating		
Sample	X	Y	Rock	Mineral analyzed	Age (ka)	Mineral analyzed	Age (ka)	Rock unit
HK-14-08	662393	2175352	Rhyolite	Zircon	44.8 ± 1.7	–	–	Qr1 Rhyolite
HK-14-10	666653	2174721	Rhyolite	Zircon	74.2 ± 4.4–4.5	–	–	Qr1 Rhyolite
HK-14–21	653766	2175788	Rhyolite	Zircon	270 ± 17–15	–	–	Qr3 rhyolitic domes
HK-14–32	671168	2188623	Rhyolite	Zircon	>350	Plagioclase	–	Qr3 rhyolitic domes
HK-14–43	655591	2187477	Rhyolite	Zircon	155.7 ± 4.6–4.9	–	–	Qr3 rhyolitic domes
HJ-14–35	656849	2178432	Rhyolite	Zircon	>350	–	–	Qr3 rhyolitic domes
HJ-14–47	667734	2187277	Rhyolite	–	–	Plagioclase	50.7 ± 4.4	Qr1 rhyolite
HJ-14–51	672524	2189054	Rhyolite	Zircon	>350	–	–	Qr3 rhyolitic domes
HJ-15-05	656849	2178432	Rhyolite	Zircon	>350	Plagioclase	693.0 ± 1.9	Qr3 rhyolitic domes
HJ-15-06	668241	2166910	Rhyolite	Zircon	–	Plagioclase	486.5 ± 2.4	Qr4 precaldera rhyolites
LH-15-01	666983	2175180	Pumice	–	–	Plagioclase	69 ± 16	QigZ Zaragoza ignimbrite
LH-15-03	674359	2184836	Ignimbrite	Zircon	180 ± 13	Plagioclase	–	QigX Xaltipan ignimbrite
LH-15-04a	689438	2169308	Ignimbrite	Zircon	160.3 ± 15.1	Plagioclase	153 ± 13	QigX Xaltipan ignimbrite
LH-15-04b	689390	2169260	Pumice	–	–	Plagioclase	70 ± 23	QtF Toba Faby
16–28a	644085	2180113	Ignimbrite	Zircon	158.4 ± 8.3	–	–	QigX Xaltipan ignimbrite

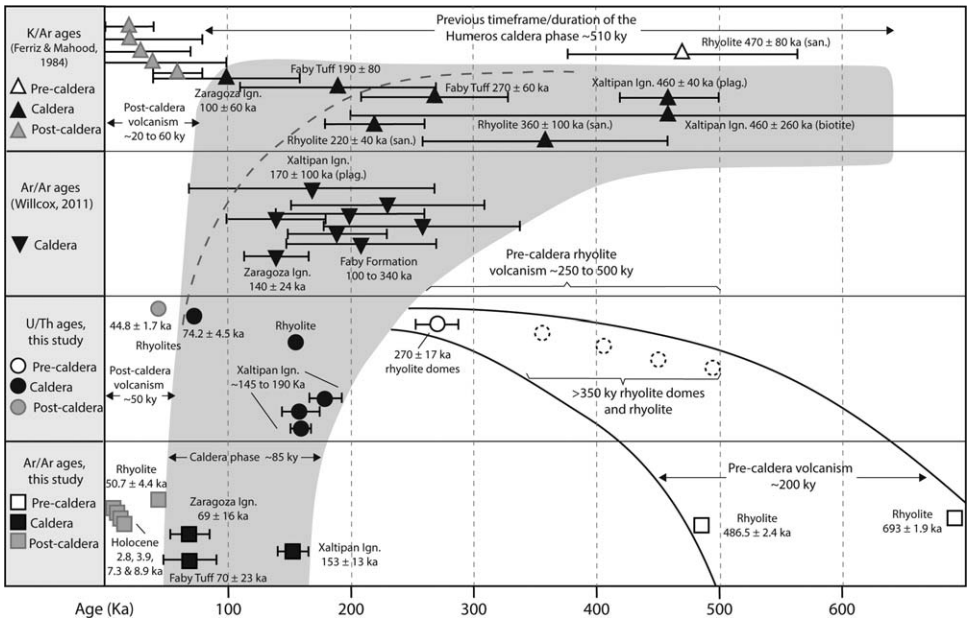

Figure 6. Schematic plot showing the ages of main units grouped in volcanic stages (precaldera, caldera, and postcaldera). Data include the new Ar/Ar and U/Th ages presented in this study, as well as recent Ar/Ar ages from Willcox (2011) and the old K-Ar time frame from Ferriz and Mahood (1984). The grey shade represents the reduction in time of the caldera stage from nearly 410 to 85 kyr. Precaldera volcanism is also shown as a group of protracted, long-lived silicic effusive events from the precaldera stage volcanism (note that in some cases the age-uncertainty can be smaller than the symbol size). Dashed circles for >350 kyr rhyolitic domes and rhyolites were not precisely determined by U/Th.

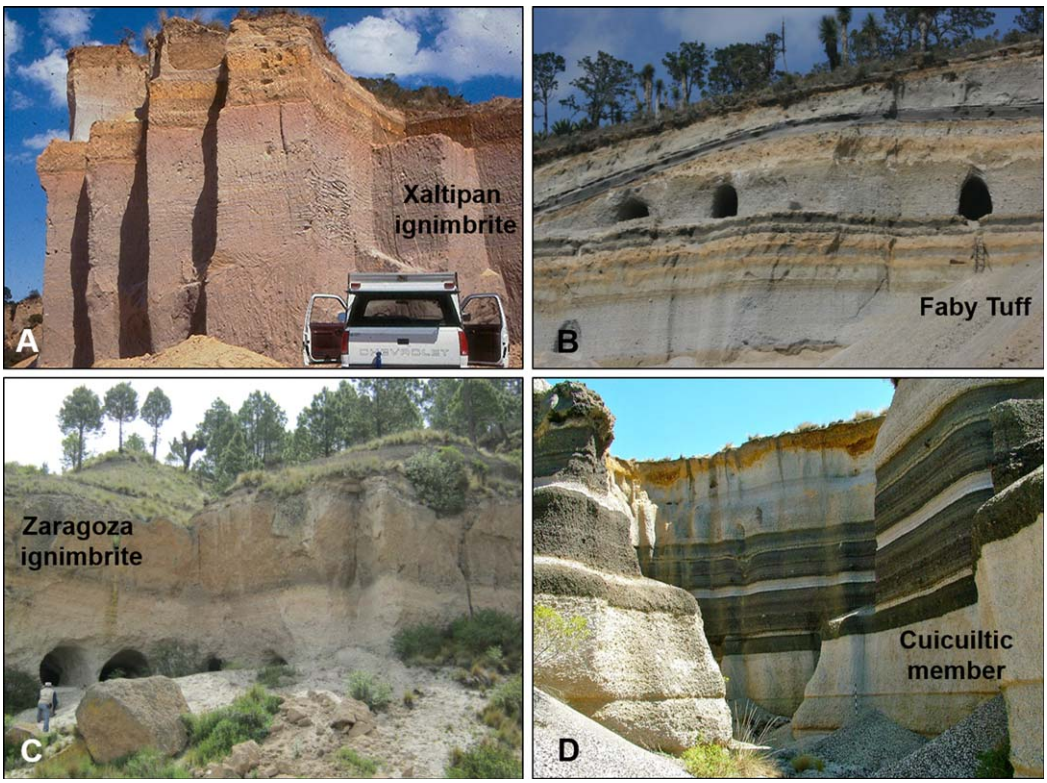

Figure 7. Selected photographs of the main explosive events associated with the evolution of Los Humeros caldera. (a) Xaltipan ignimbrite; (b) Faby Tuff; (c) Zaragoza ignimbrite; (d) Cuicuiltic member.

3.2.3. Caldera-Forming Phase 2 (Zaragoza)

The smaller, 9–10 km wide, and younger Los Potreros caldera is associated with the emplacement of the compositionally zoned rhyodacitic to andesitic Zaragoza ignimbrite (Carrasco-Núñez et al., 2012), an intraplinian pyroclastic flow deposit (Figure 7c), with a volume of ~15 km^3 DRE (Carrasco-Núñez & Branney, 2005). The new 69 ± 16 ka $^{40}Ar/^{39}Ar$ date proposed in this paper is much younger than the previous $^{40}Ar/^{39}Ar$ age of 140 ± 24 ka obtained by Willcox (2011; Figure 8). The proposed age for the Zaragoza ignimbrite is supported by the age of 74.2 ± 4.5 ka (U/Th, zircon) of an underlying rhyodacitic lava flow in an outcrop along the Los Potreros scarp (see Figure 2 for location).

Even though the ages obtained for the Faby Tuffs and the Zaragoza ignimbrite are quite close at around 70 ka, and might suggest that the Faby Tuff represents a succession of Plinian eruptions that record the precursory build-up of the climactic Zaragoza caldera-forming phase, field evidence suggests that they are two separate eruptive phases.

3.3. Postcaldera Stage

This stage includes a late Pleistocene resurgent phase, followed by a Holocene ring-fracture and bimodal phase that was previously considered to be loosely constrained between 40 and 20 ka, and part of that referred as younger than 20 ka, based on imprecise K-Ar data (Ferriz & Mahood, 1984).

3.3.1. Resurgent Phase

Rhyolitic and dacitic magmas erupted after the caldera stage in the central part of the caldera, located right in the middle of the active geothermal field. The U/Th zircon age of 44.8 ± 1.7 ka is slightly younger than the previously reported K-Ar date (60 ± 20 ka; Ferriz & Mahood, 1984). In addition, a rhyolitic dome formed outside of the caldera toward the north has been now dated at 50.7 ± 4.4 ka ($^{40}Ar/^{39}Ar$, plagioclase). This activity was followed by explosive eruptions, producing dacitic pumice fall units (Xoxoctic Tuff, 0.6 km^3 at ~50 ka) and pyroclastic flows and breccia deposits (Llano Tuff; Ferriz & Mahood, 1984; Willcox, 2011), with a minimum age of about 28.3 ± 1.1 ka (C^{14}, cal years B.P. 30,630–29,745; Rojas-Ortega, 2016).

3.3.2. Ring-Fracture and Bimodal Phase

The youngest, Holocene extensive eruptive phase occurred toward the south, north, and central part of Los Humeros caldera, which is dominated by effusive andesitic and basaltic andesite volcanism related mainly to ring-fractures of the older Los Humeros caldera, with also some explosive phases erupting both basaltic andesite and rhyodacitic tephras. Most of the effusive activity was considered to be between 40 and 20 ka (Ferriz & Mahood, 1984; Figure 8). However, the uncertainties on all of these 40–20 ka K/Ar dates are ±100% or greater, and thus these ages are not reliable. Recent ^{14}C dating presented in a companion paper (Carrasco-Núñez et al., 2017a) place the most recent activity at LHVC within the Holocene. Andesitic basalts and trachyandesitic lavas erupted to the north of the LHVC at about 8.9 ± 0.03 ka (cal years B.P. 10,185–9,910, Carrasco-Núñez et al., 2017a). After this mostly effusive episode, a contemporaneous bimodal explosive/effusive activity produced the Cuicuiltic member at 7.3 ± 0.1 ka (cal years B.P. 7,982–8,371; Dávila-Harris & Carrasco-Núñez, 2014), a rhythmic alternation of trachyandesitic, and basaltic fall layers (Figure 7d), formerly associated with the formation of the Xalapazco crater (Figure 2; Ferriz & Mahood, 1984). The most recent activity comprises ring-fracture trachyandesite and olivine-bearing basaltic lava flows (Figure 8) erupted at 3.9 ± 0.13 ka (cal years B.P. 3,933–3,940, 3,971–4,653; Carrasco-Núñez et al., 2017a), as well as trachytic lava flows erupted near the SW caldera rim, at 2.8 ± 0.03 ka (cal years B.P. 3,065–2,920, 2,910–2,880; Carrasco-Núñez et al., 2017a).

3.4. Implications on the Longevity and Magma Storage of LHVC

Large calderas are associated with long-lasting magmatic systems, which are on the order of a few millions of years, as for instance: Yellowstone (Christiansen, 2001), Cascade calderas (Hughes & Mahood, 2011), Okataina Volcanic Centre, New Zealand (Cole et al., 2014). The concept of long time scales were inferred in earlier studies of Long Valley (Reid & Coath, 2000; Reid et al., 1997) and have evolved to a more complex model of prolonged crustal storage tapping different parts of a mush or crystalline zone with the ephemeral formation of a magma reservoir that eventually erupt (Bachmann, 2010; Bachmann & Bergantz, 2008; Cashman & Giordano, 2014; Chamberlain et al., 2014; Cooper & Kent, 2014; Hildreth, 2004; Hildreth & Wilson, 2007; Lipman, 2007; Reid, 2008; Reid et al., 2011). The successive caldera-collapse forming multiple calderas (Los Humeros and Los Potreros) likely developed variously overlapping, nested, reactivated, and overprinted structures shaping the feeding system (Gudmundsson, 2012). The magmatic system beneath Los Humeros

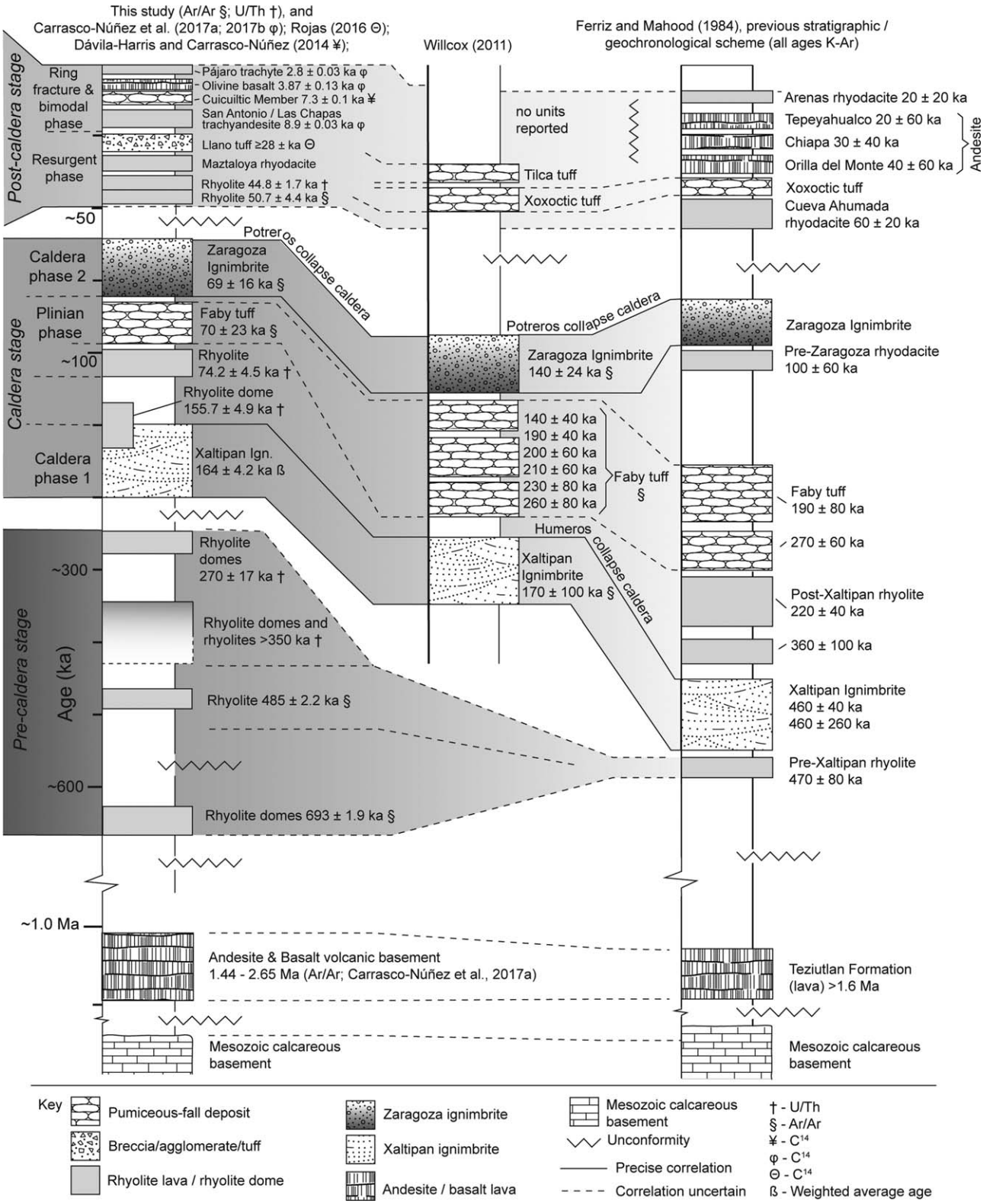

Figure 8. Previous and new developed stratigraphic framework for the volcanic units exposed at LHVC, based on Ar/Ar and U/Th geochronology (this study) and C^{14} for Holocene units (Dávila-Harris and Carrasco-Núñez, 2014; Carrasco-Núñez et al., 2017a, 2017b; Norini et al., 2015; Rojas-Ortega, 2016). Central column data are mainly Ar/Ar from Willcox (2011). Far right column represents the old stratigraphic context based on K-Ar ages from Ferriz and Mahood (1984). Vertical age scale and lithologic units are schematic. Data of Ferriz and Mahood (1984) were originally reported with 1σ uncertainties. It is reported with 2σ uncertainties here.

is likely complex and irregular with active melt zones and partially crystallized zones where mixing and mingling of hybrid magmas erupted during the Zaragoza ignimbrite eruption (Carrasco-Núñez et al., 2012).

The new U/Th and $^{40}Ar/^{39}Ar$ dates reported in this paper have important implications on the expected longevity of the Los Humeros magmatic system because our results indicate that this is a very young system (164.0 $\pm$ 4.2 ka and younger; Figure 8) whose lifetime is expected to last much longer into the future than previously considered based on the previous caldera-forming age of 460 ka (Figure 8). This is particularly important because the associated geothermal system is also expected to be younger, so the geothermal potential must be reassessed considering this key point.

Our combined U/Th and $^{40}Ar/^{39}Ar$ dating of the Xaltipan ignimbrite, and its excellent agreement with data from recent reports (Aliaga-Campuzano et al., 2017; Willcox, 2011), represent compelling evidence indicating that the collapse of Los Humeros Caldera and the emplacement of the Xaltipan ignimbrite occurred nearly 300 kyr later than initially suggested by Ferriz and Mahood (1984). Furthermore, the excellent correspondence between the majority of the zircon U/Th ages and the plagioclase Ar-Ar ages (meaning time between crystallization and eruption) suggests that the time for the assembly of the magma before the eruption of the Xaltipan ignimbrite was likely short, probably around 5 ka, possibly due to relatively high magma flux. Although large caldera-forming eruptions apparently involve long times required for compaction-driven melt extraction (Bachmann & Bergantz, 2004; Bachmann et al., 2007), such short time frames (5 ka) estimated for LHVC are in agreement with similar occurrences elsewhere (e.g., Bishop [Wark et al., 2007]; Oruanui [Allan et al., 2013]; Wakamaru [Saunders et al., 2010]; Yellowstone [Bindeman et al., 2008; Matthews et al., 2015; Rivera et al., 2014; Wotzlaw et al., 2014, 2015]), indicating very fast magma storage and extraction rates from parent crystal mushes.

The Xaltipan ignimbrite represents the climax of volcanism at Los Humeros and is likely preceded by a peak in magma production rate consistent with numerical simulations of conductive cooling models of igneous bodies, magma production rates, and intrusive to extrusive ratios (Costa, 2008). In particular, we suggest that rapid buildup of eruptible magma can be explained by magma extraction from the parent crystal mush induced by injection of new magma (e.g., Bachmann & Bergantz, 2004; Reid et al., 2011), which can be segregated from more crystalline parts of a magmatic reservoir by channels or dikes during a rapid interconnection of isolated melt lenses (e.g., Eichelberger & Izbekov, 2000). That injection is supported by the repeated occurrence in the LHVC stratigraphic record of recharge magma, in the form of basalts or hybrids (andesites).

We also have been able to reconstruct a much longer duration for the precaldera silica-rich volcanism, which likely testifies to the buildup preceding the caldera stage. The oldest rhyolites for the precaldera stage are dated around 683.0 $\pm$ 1.7 ka and the youngest at 270 $\pm$ 15 ka, which mark a total duration of $\sim$400 kyr before the first large explosive eruptions (ignimbrite-forming scale). The new data set also provides interesting contributions to the present evolutionary stage of the caldera. Previously, the post caldera volcanism was believed to have lasted $\sim$40 kyr from 60 to 20 ka (Ferriz & Mahood, 1984). Our new ages constrain the beginning of the postcaldera stage to 50 ka, with the youngest Holocene activity at 4 ka. Within this 50 kyr of postcaldera evolution, the compositions have changed from rhyodacitic and dacitic tuffs to basaltic andesitic and basaltic olivine-bearing lavas. This heterogeneous magmatic production from Los Humeros most recent stage could reflect complex conditions at depth and the presence of recharge magma interacting with a resident reservoir, which could raise the possibility of future (explosive?) eruptions. The simultaneous presence of basaltic recharge melts could indicate replenishment of the reservoir that represents both a volcanic hazard and also an extended geothermal potential.

3.5. Implications for Geothermal Exploration

Large silicic collapse calderas usually host active hydrothermal systems with a lifetime of 1–2 or even more million years after the final volcanic activity (Kolstad & McGetchin, 1978), depending of the extent of permeable zones. Geothermal reservoirs form above the complex mush-like crystallizing magma reservoirs, in which fluids from shallow or deep aquifers are heated, pressurized, and contaminated by magmatic volatiles, and ascend convectively in fracture networks within the caldera (Duffield & Sass, 2003).

Previous estimates of the amount of erupted material has been calculated at about 1/3 to 1/10 of the partly molten magmatic reservoir below calderas larger than 10 km diameter, which cool slowly and may be heat

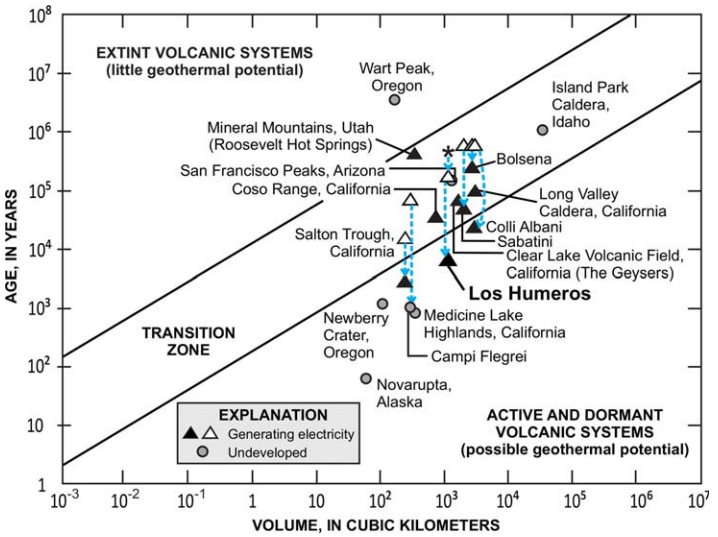

Figure 9. Age versus volume of magma reservoir, derived from conductive models of selected geothermal fields and volcanic systems. The lower boundary of the transitional zone implies heat transfer effects of convection within the magmatic reservoir, while the upper boundary considers magmatic systems that cool to near ambient temperatures, with much lower heat capacity (modified after Smith & Shaw, 1975; Duffield & Sass, 2003). Solid triangles represent the youngest (rhyolitic) eruption of a magmatic system, when accompanied with an empty triangle, this represents the onset of the magmatic system, and the blue dashed lines point to the evolution age to the youngest activity. The asterisk indicates the previous proposed age (460 ka) for LHVC.

sources for up to 2×10^6 years (Smith & Shaw, 1975). A conventional estimation of 10% the volume of the eruptive products in relation to the volume of the underlying magma reservoir has been established (Smith, 1979; Smith & Shaw, 1975, 1979). According to this approximate model, the magmatic reservoir for Los Humeros can be estimated in more than 1,150 km^3, which is in agreement with the thermal numerical estimation made by Verma et al. (2011), in the range of 1,000–1,400 km^3.

A rough estimation of the amount of heat carried by the hydrothermal fluids ranges from 1 to 10% according to average porosities of the geothermal reservoirs (e.g., Muffler & Cataldi, 1978; Smith & Shaw, 1975). These estimations have important implications in the exploration for geothermal heat sources because by using eruption age constraints, cooling models can predict the residual heat left in the magmatic reservoir. Classical conductive models of heat resource consider that the heat production capacity is a function of the age of the most recent activity and the volume of magma bodies (Duffield & Sass, 2003; Smith & Shaw, 1975), which implies that a larger, younger magma reservoir is more likely to have a productive geothermal field. The new geochronologic data set presented here shows much younger ages for the onset of the Los Humeros caldera activity (164 ka), and this has very important implications on the thermal conditions of the system envisaging more heat and higher geothermal potential (Figure 9). Los Humeros moves from the transitional zone to the zone of active systems when considering the most recent rhyolitic activity (<7.3 ka; Dávila-Harris & Carrasco-Núñez, 2014). It falls along a trend formed by some important geothermal fields such as the Geysers, Salton Trough, Coso Range, and Long Valley caldera, all in California (USA) (Duffield & Sass, 2003) as well as Bolsena, Colli Albani, and Sabatini in Italy (Doveri et al., 2010; Giordano et al., 2014). Some other younger systems such as Novarupta, Newberry crater, Medicine Lake, and Campi Flegrei (Wohletz et al., 1999, Duffield & Sass, 2003) are currently undeveloped fields (Figure 9); however, they represent very favorable heat capacity for future geothermal exploitation.

In addition to the age and volume of the magma body, other factors are critical in determining geothermal potential of an area, like the depth of the magma reservoir and the porosity and permeability of the overlying rock volume. In the case of Los Humeros, a recent study using silica melt inclusions reveals volatile saturation pressures between 1.2 and 1.4 kbars, which corresponds to a depth of ~5 km (Creon et al., 2016), consistent with a previous estimation of 5–10 km (Verma et al., 2011). The geothermal reservoir is located on average at 1,400 m deep within the thick andesitic precaldera unit, where the permeability is apparently controlled by a NW-SE and E-W structural system (i.e., Cedillo, 1997; Gutiérrez-Negrín & Izquierdo-Montalvo, 2010; Norini et al., 2015). However, hydrothermal fluid migration is highly dependent of lateral lithofacies variations associated with the stratigraphic complexity at the subsurface (Carrasco-Núñez et al., 2017a, 2017b) and perhaps also due to microporosity in the volcanic rocks (Cid et al., 2017).

It must be noted that the short time scales (~5 kyr) of magma assembly before the eruption of the caldera forming Xaltipan and Zaragoza ignimbrites, suggested by paired U/Th and Ar/Ar age determinations, is indicative of rejuvenation of the system due to recharge magmas. The general implication for the application to geothermal systems of heat conduction models is that they should take into account not just the age of the latest caldera-forming event but also the evidence and timing for rejuvenation. At LHVC, for example, the most recent Holocene phase is dominated by bimodal volcanism and eruption of basaltic magmas from the outer ring-faults of the old LH caldera. We interpret this as an evidence of current rejuvenation of the system, which may better explain its high enthalpy (up to about 400°C) at shallow depths respect to models associated with pure heat conduction released from the LHVC magma chamber.

4. Conclusions

LHVC has been active from the middle Pleistocene to the Holocene. Recent developments in geochronologic methods allow more precise and accurate temporal constraints during this period. In this paper, we have used two different geochronometers (zircon U/Th and plagioclase $^{40}Ar/^{39}Ar$) to establish a much younger onset of the caldera-forming volcanism at LHVC than previously reported (from 460 ± 40 ka versus 164 ± 4.2 ka, Xaltipan ignimbrite). Younger parts of the stratigraphy have also been dated, and the results are in agreement with the new time scale framework. For example, the caldera-forming eruption at Los Humeros, related to the Zaragoza ignimbrite, has been updated to a much younger and age of 69 ± 16 ka. Therefore, the time frame for the caldera-forming stage has been refined from 410 to 94 kyr. The demonstrated rejuvenation of the magmatic system provides support to explain the observed high enthalpy of the geothermal system (up to 400°C) at shallow depths in comparison to models associated with pure heat conduction released from the LHVC magma chamber. The residence times inferred for the magma assembly of the main caldera-forming eruptions related to the LHVC are very short (∼5 kyr) for such a large magmatic system. Considering the traditional conductive models of heat resource, where the main factors are the age and the volume of the magmatic system, conditions for Los Humeros are now considered to be more favorable for heat production capacity with higher geothermal potential, in view of the large volume of the magmatic source estimated in at least 1,150 km^3 and the much younger ages of the peak of caldera volcanism.

Acknowledgments

This work was funded by project P05 of the CeMie-GEO Consortium 2007032 supported by SENER-CONACYT Sustainability Foundation, as well as PAPIIT-UNAM IN 106314. Partial support was provided by GEMEX project (grant agreements 268074 and 727550-GEMexH2020-LCE-2016–2017/H2020-LCE-2016-RES-CCS-RIA). We want to thank the critical reviews by O. Bachmann, F. Jourdan, and J. Vazquez that greatly improved the paper, as well as an anonymous reviewer and the Associated Editor Janne Blichert-Toft. Thank you to Carlos Ortega for laboratory support. Juan Vázquez, Lorena de León, Penélope López, Mario Navarro, Daniela Peña, Francisco Fernández, Steven Barrios, Gerardo Huerta, Jesús Machorro, and Nathan Andersen helped in map processing and sample preparation. We also thank the Geothermoelectric Project Management of the Electricity Federal Commission staff for support during this work, particularly to Magaly Flores and Miguel Ramírez. The data used are listed in the tables, figures, and in supporting information SI and SII.

References

Aliaga-Campuzano, M. P., López-Martínez, R., Dávila-Harris, P., Espinasa-Pereña, R., Espino-del-Castillo, A., & Bernal, J. P. (2017). Timing of speleogenesis of Las Karmidas Cave (Mexico): First description of pseudokarst in ignimbrite. *International Journal of Speleology*, *46*(3), 331–343. https://doi.org/10.5038/1827-806X.46.3.2097

Allan, A. R., Morgan, D., Wilson, C. N., & Millet, M.-A. (2013). From mush to eruption in centuries: Assembly of the super-sized, Oruanui magma body. *Contributions to Mineralogy and Petrology*, *166* (1), 143–164.

Audi, G., Bersillon, O., Blachot, J., & Wapstra, A. H. (1997). The NUBASE evaluation of nuclear and decay properties. *Nuclear Physics A*, *624*(1), 1–124.

Bachmann, O. (2010). The petrologic evolution and pre-eruptive conditions of the rhyolitic Kos Plateau Tuff (Aegean arc). *Central European Journal of Geosciences*, *2*(3), 270–305.

Bachmann, O., & Bergantz, G. W. (2004). On the origin of crystal-poor rhyolites: Extracted from batholithic crystal mushes. *Journal of Petrology*, *45*(8), 1565–1582.

Bachmann, O., & Bergantz, G. W. (2008). Rhyolites and their source mushes across tectonic settings. *Journal of Petrology*, *49*(12), 2277–2285.

Bachmann, O., Oberli, F., Dungan, M. A., Meier, M., Mundil, R., & Fischer, H. (2007). $^{40}Ar/^{39}Ar$ and U–Pb dating of the Fish Canyon magmatic system, San Juan Volcanic field, Colorado: Evidence for an extended crystallization history. *Chemical Geology*, *236*(1–2), 134–166.

Bachmann, O., Schoene, B., Schnyder, C., & Spikings, R. (2010). 40Ar/39Ar and U/Pb dating of young rhyolites in the Kos-Nisyros volcanic complex, Eastern Aegean Arc (Greece): Age discordance due to excess 40Ar in biotite. *Geochemistry, Geophysics, Geosystems*, *11*, Q0AA08. https://doi.org/10.1029/2010GC003073

Barboni, M., Boehnke, P., Schmitt, A. K., Harrison, T. M., Shane, P., Bouvier, A.-S., & Baumgartner, L. (2016). Warm storage for arc magmas. *Proceedings of the National Academy of Sciences of the United States of America*, *113*(49), 13959–13964.

Bernal, J. P., Solari, L. A., Gómez-Tuena, A., Ortega-Obregón, C., Mori, L., Vega-González, M., & Espinosa-Arbeláez, D. G. (2014). *In-situ* $^{230}Th/U$ dating of Quaternary zircons using LA-MCICPMS, *Quaternary Geochronology*, *23*(10), 46–55.

Bindeman, I. N., Fu, B., Kita, N. T., & Valley, J. W. (2008). Origin and evolution of silicic magmatism at Yellowstone based on ion microprobe analysis of isotopically zoned zircons. *Journal of Petrology*, *49*(1), 163–193.

Boehnke, P., Barboni, M., & Bell, E. A. (2016). Zircon U/Th model ages in the presence of melt heterogeneity. *Quaternary Geochronology*, *34*, 69–74.

Branney, M. J. (1995). Downsag and extension at calderas: New perspectives on collapse geometries from ice-melt, mining, and volcanic subsidence. *Bulletin of Volcanology*, *57*(5), 303–318.

Brown, S., & Fletcher, I. R. (1999). SHRIMP U-Pb dating of the preeruption growth history of zircons from the 340 ka Whakamaru Ignimbrite, New Zealand: Evidence for >250 ky magma residence times. *Geology*, *27*(11), 1035–1038.

Carrasco-Núñez, G., Arzate, J., Bernal, J. P., Carrera, J., Cedillo, F., Dávila-Harris, P., . . . Willcox, C. (2015). A new geothermal exploration program at Los Humeros volcanic and geothermal field (Eastern Mexican Volcanic Belt). Paper presented at Proceedings of World Geothermal Congress 2015, Melbourne, Australia, April 19–25.

Carrasco-Núñez, G., & Branney, M. (2005). Progressive assembly of a massive layer of ignimbrite with normal-to-reverse compositional zoning: The Zaragoza ignimbrite of central Mexico. *Bulletin of Volcanology*, *68*(1), 3–20.

Carrasco-Núñez, G., Gómez-Tuena, A., & Lozano, L. (1997). *Geologic map of Cerro Grande volcano and surrounding area, Central México*. *Maps and Charts Series* (MCH 081, p 10). Boulder, CO: Geological Society of America.

Carrasco-Núñez, G., Hernández, J., De León, L., Dávila, P., Norini, G., Bernal, J. P., . . . López, P. (2017a). Geologic map of Los Humeros volcanic complex and geothermal field, eastern Trans-Mexican Volcanic Belt. *Terra Digitalis*, *1*(2), 1–11.

Carrasco-Núñez, G., López-Martínez, M., Hernández, J., & Vargas, V. (2017b). Subsurface stratigraphy and its correlation with the surficial geology at Los Humeros geothermal field, eastern Trans-Mexican Volcanic Belt. *Geothermics*, *67*, 1–17.

Carrasco-Núñez, G., McCurry, M., Branney, M. J., Norry, M., & Willcox, C. (2012). Complex magma mixing, mingling, and withdrawal associated with an intraplinian ignimbrite eruption at a large silicic caldera volcano: Los Humeros of central Mexico. *Geological Society of America Bulletin*, *124*(11–12), 1793–1809.

Cashman, K. V., & Giordano, G. (2014). Calderas and magma reservoirs. *Journal of Volcanology and Geothermal Research*, *288*, 28–45.
Cashman, K. V., Spark, R. S. J., & Blundy, J. D. (2017). Vertically extensive and unstable magmatic systems: A unified view of igneous processes. *Science*, *355*(6331), eaag3055, https://doi.org/10.1126/science.aag3055
Cedillo, F. (1997). *Geología del subsuelo del campo geotérmico de Los Humeros, Pue* (Internal Rep. HU/RE/03/97, pp. 30). Mexico City: Comisión Federal de Electricidad.
Chamberlain, K. J., Wilson, C. J. N., Wooden, J. L., Charlier, B. L. A., & Ireland, T. R. (2014). New perspectives on the Bishop Tuff from Zircon Textures, Ages and Trace Elements. *Journal of Petrology*, *55*, 355–426.
Cheng, H., Lawrence Edwards, R., Shen, C.-C., Polyak, V. J., Asmerom, Y., Woodhead, J., . . . Calvin Alexander, E., Jr. (2013). Improvements in 230Th dating, 230Th and 234U half-life values, and U–Th isotopic measurements by multi-collector inductively coupled plasma mass spectrometry. *Earth and Planetary Science Letters*, *371–372*, 82–91.
Christiansen, R. L. (2001). The Quaternary and Pliocene yellowstone plateau volcanic field of Wyoming, Idaho, and Montana. *U. S. Geological Survey Professional Paper*, *729-G*.
Cid, H. E., Carrasco-Núñez, G., & Manea, V. C. (2017). Improved method for effective rock microporosity estimation using X-ray microtomography. *Micron*, *97*, 11–21.
Cole, J. W., Deering, C., Burt, R., Sewell, S., Shane, P., & Matthews, N. (2014). Okataina volcanic centre, Taupo volcanic zone, New Zealand: A review of volcanism and synchronous pluton development in an active, dominantly silicic caldera system. *Earth-Science Reviews*, *128*, 1–17.
Cole, J. W., Milner, D. M., & Spinks, K. D. (2005). Calderas and caldera structures: A review. *Earth-Science Reviews*, *69*(1–2), 1–26.
Cooper, G. F., Wilson, C. J. N., Millet, M. A., Baker, J. A., & Smith, E. G. C. (2012). Systematic tapping of independent magma chambers during the 1 Ma Kidnappers supereruption. *Earth and Planetary Science Letters*, *313–314*, 23–33.
Cooper, K. M., & Kent, A. J. R. (2014). Rapid remobilization of magmatic crystals kept in cold Storage. *Nature*, *506*(7489), 480–483. https://doi.org/10.1038/nature12991
Costa, F. (2008). Residence times of silicic magmas associated with calderas. In J. Gottsmann & J. Martì (Eds.), *Developments in volcanology* (Vol. 10, pp. 1–55). Amsterdam, the Netherlands: Elsevier.
Creon, L., Levresse, G., & Carrasco-Núñez, G. (2016). New approach on volatile contents determination in silicate melt inclusions: A coupling X-ray microtomography and geochemical approach in Los Humeros caldera complex (Eastern Mexican Volcanic Belt). Abstract #V31A-3058 presented at 2016 Fall Meeting, AGU, San Francisco, CA.
Dávila-Harris, P., & Carrasco-Núñez, G. (2014). An unusual syn-eruptive bimodal eruption: The Holocene Cuicuiltic Member at Los Humeros caldera, Mexico. *Journal of Volcanology and Geothermal Research*, *271*, 24–42.
Deering, C. D., Keller, B., Schoene, B., Bachmann, O., Beane, R., & Ovtcharova, M. (2016). Zircon record of the pluton-volcanic connection and protracted rhyolite melt evolution. *Geology*, *44*(4), 267–270.
De la Cruz, V. (1983). *Estudio geológico a detalle de la zona geotérmica Los Humeros, Puebla*. (Internal Rep. 10/83, pp. 51). Mexico City: Comisión Federal de Electricidad.
Doveri, M., Lelli, M., Marini, L., & Raco, B. (2010). Revision, calibration, and application of the volume method to evaluate the geothermal potential of some recent volcanic areas of Latium, Italy. *Geothermics*, *39*(3), 260–269.
Druitt, T. H., & Sparks, R. S. J. (1984). On the formation of calderas during ignimbrite eruptions. *Nature*, *310* (5979), 679–681.
Duffield, W., & Sass, J. (2003). *Geothermal energy—Clean power from the Earth's heat* (Circular 1249, p. 34). Reston, VA: U.S. Geothermal Development, U.S. Geological Survey.
Eichelberger, J. C., & Izbekov, P. E. (2000). Eruption of andesite triggered by dyke injection: Contrasting cases at Karymsky Volcano, Kamchatka and Mt Katmai, Alaska. *Philosophical Transactions of the Royal Society of London A: Mathematical, Physical and Engineering Sciences*, *358*(1770), 1465–1485.
Ellis, B. S., Barry, T., Branney, M. J., Wolff, J. A., Bindeman, I., Wilson, R., & Bonnichsen, B. (2010). Petrologic constraints on the development of a large-volume, high temperature, silicicmagma system: The Twin Falls eruptive centre, central Snake River Plain. *Lithos*, *120*(3–4), 475–489.
Ellis, B. S., Mark, D. F., Troch, J., Bachmann, O., Guillong, M., Kent, A. J. R., & von Quadt, A. (2017). Split-grain 40Ar/39Ar dating: Integrating temporal and geochemical data from crystal cargoes. *Chemical Geology*, *457*, 15–23. https://doi.org/10.1016/j.chemgeo.2017.03.005
Ferriz, H., & Mahood, G. (1984). Eruption rates and compositional trends at Los Humeros Volcanic Center, Puebla, Mexico. *Journal of Geophysical Research*, *89*(B10), 8511–8524.
Ferriz, H., & Mahood, G. (1987). Strong compositional zonation in silicic magmatic system: Los Humeros, Mexican Neovolcanic Belt. *Journal of Petrology*, *28*(1), 171–209.
Gardner, J. E., Layer, P. W., & Rutherford, M. J. (2002). Phenocrysts versus xenocrysts in the youngest Toba Tuff: Implications for the petrogenesis of 2800 km^3 of magma. *Geology*, *30*(4), 347–350.
Geshi, N., Ruch, J., & Acocella, V. (2014). Evaluating volumes for magma chambers and magma withdrawn for caldera collapse. *Earth and Planetary Science Letters*, *396*, 107–115.
Geyer, A., Folch, A., & Martí, J. (2006). Relationship between caldera collapse and magma chamber withdrawal: An experimental approach. *Journal of Volcanology and Geothermal Research*, *157*(4), 375–386.
Giordano, G., De Benedetti, A. A., Bonamico, A., Ramazzotti, P., & Mattei, M. (2014). Incorporating surface indicators of reservoir permeability into reservoir volume calculations: Application to the Colli Albani caldera and the Central Italy Geothermal Province. *Earth-Science Reviews*, *128*, 75–92.
Gómez-Tuena, A., & Carrasco-Núñez, G. (2000). Cerro Grande volcano: The evolution of a Miocene stratocone in the early Trans-Mexican Volcanic Belt. *Tectonophysics*, *318*(1–4), 249–280.
Gualda, G. A. R., & Ghiorso, M. S. (2013). The Bishop Tuff giant magma body: An alternative to the Standard Model. *Contributions to Mineralogy and Petrology*, *166*(3), 755–775.
Gudmundsson, A. (2012). Magma chambers: Formation, local stresses, excess pressures, and compartments. *Journal of Volcanology and Geothermal Research*, *237–238*, 19–41.
Gutiérrez-Negrín, L., & Izquierdo-Montalvo, G. (2010). Review and update of the main features of the Los Humeros geothermal field, Mexico. Paper presented at Proceedings World Geothermal Congress 2010, Bali, Indonesia.
Heizler, M. T., Perry, F. V., Crowe, B. M., Peters, L., & Appelt, R. (1999). The age of Lathrop Wells volcanic center: A $^{40}Ar/^{39}Ar$ dating investigation. *Journal of Geophysical Research*, *104*(B1), 767–804.
Hildreth, W. (2004). Volcanological perspectives on long Valley Mammoth Mountain, and Mono Craters: Several contiguous but discrete systems. *Journal of Volcanology and Geothermal Research*, *136*(3–4), 169–198.
Hildreth, W., & Wilson, C. J. N. (2007). Compositional zoning of the Bishop Tuff. *Journal of Petrology*, *48*(5), 951–999.

Hughes, G. R., & Mahood, G. A. (2011). Silicic calderas in arc settings: Characteristics, distribution, and tectonic controls. *Geological Society of America Bulletin*, *123*(7–8), 1577–1595.

Jaffey, A. H., Flynn, K. F., Glendenin, L. E., Bentley, W. C., & Essling, A. M. (1971). Precision measurement of half-lives and specific activities of ^{235}U and ^{238}U. *Physical Review C*, *4*(5), 1889–1906.

Jicha, B. R., Singer, B. S., & Sobol, P. (2016). Re-evaluation of the ages of ^{40}Ar/^{39}Ar sanidine standards and supereruptions in the western U.S. using a Noblesse multi-collector mass spectrometer. *Chemical Geology*, *431*, 54–66.

Kolstad, C. D., & McGetchin, T. R. (1978). Thermal evolution models for the Valles caldera with reference to a hot-dry-rock geothermal experiment. *Journal of Volcanology and Geothermal Research*, *3*(1–2), 197–218.

Lipman, P. W. (1997). Subsidence of ash-flow calderas: Relation to caldera size and magma chamber geometry. *Bulletin of Volcanology*, *59*(3), 198–218.

Lipman, P. W. (2007). Incremental assembly and prolonged consolidation of Cordilleran magma chambers: Evidence from the Southern Rocky Mountain volcanic field. *Geosphere*, *3*(1), 42–70.

Ludwig, K. R. (2012). *User's manual for Isoplot 3.75: A geochronological toolkit for Microsoft Excel*, *Berkeley Geochronology Center Special Publication No. 5*. Berkeley, CA: Berkeley Geochronology Center.

Ludwig, K. R., & Titterington, D. M. (1994). Calculation of ^{230}Th/U isochrons, ages and errors. *Geochimica et Cosmochimica Acta*, *58*(22), 5031–5042.

Martí, J. (1991). Caldera-like structures related to Permo-Carboniferous volcanism of the Catalan Pyrenees (NE Spain). *Journal of Volcanology and Geothermal Research*, *45*(3–4), 173–186.

Matthews, N. E., Vazquez, J. A., & Calvert, A. T. (2015). Age of the Lava Creek supereruption and magma chamber assembly at Yellowstone based on ^{40}Ar/^{39}Ar and U-Pb dating of sanidine and zircon crystals. *Geochemistry, Geophysics, Geosystems*, *16*, 2508–2528. https://doi.org/10.1002/2015GC005881

Min, K., Mundil, R., Renne, P. R., & Ludwig, K. R. (2000). A test for systematic errors in ^{40}Ar/^{39}Ar geochronology through comparison with U/Pb analysis of a 1.1-Ga rhyolite. *Geochimica et Cosmochimica Acta*, *64*(1), 73–98.

Muffler, L. J. P., & Cataldi, R. (1978). Methods for regional assessment of geothermal resources. *Geothermics*, *7*(2–4), 53–89. https://doi.org/10.1016/0375-6505(78)90002-0

Müller, W., Shelley, M., Miller, P., & Broude, S. (2009). Initial performance metrics of a new custom-designe ArF xcimer La-ICPMS system coupled to a two-volume laser-ablation cell. *Journal of Analytical Atomic Spectrometry*, *24*(2), 209–214.

Niespolo, E. M., Rutte, D., Deino, A. L., & Renne, P. R. (2017). Intercalibration and age of the Alder Creek sanidine ^{40}Ar/^{39}Ar standard. *Quaternary Geochronology*, *39*, 205–213. https://doi.org/10.1016/j.quageo.2016.09.004

Norini, G., Groppelli, G., Sulpizio, R., Carrasco-Núñez, G., Davila-Harris, P., Pellicioli, C., . . . De Franco, R. (2015). Structural analysis and thermal remote sensing of the Los Humeros Volcanic Complex: Implications for volcano structure and geothermal exploration. *Journal of Volcanology and Geothermal Research*, *301*, 221–237.

Paton, C., Hellstrom, J., Paul, B., Woodhead, J., & Hergt, J. (2011). Iolite: Freeware for the visualisation and processing of mass spectrometric data. *Journal of Analytical Atomic Spectrometry*, *26*(12), 2508–2518.

Perez-Reynoso, J. (1978). Geología y petrografía de Los Humeros. *Geomimet*, *91*, 97–106.

Reid, M. R. (2008). How long does it take to supersize an eruption? *Elements*, *4*(1), 23–28.

Reid, M. R., & Coath, C. D. (2000). *In situ* U-Pb ages of zircons from the Bishop Tuff: No evidence for long crystal residence times. *Geology*, *28*(5), 433–446.

Reid, M. R., Coath, C. D., Harrison, T. M., & McKeegan, K. D. (1997). Prolonged residence times for the youngest rhyolites associated with Long Valley Caldera: ^{230}Th-^{238}U ion microprobe dating of young zircons. *Earth and Planetary Science Letters*, *150*(1–2), 27–39.

Reid, M. R., Vazquez, J. A., & Schmitt, A. K. (2011). Zircon-scale insights into the history of a Supervolcano, Bishop Tuff, Long Valley, California, with implications for the Ti-in-zircon geothermometer. *Contributions to Mineralogy and Petrology*, *161*(2), 293–311.

Rivera, T. A., Schmitz, M. D., Crowley, J. L., & Storey, M. (2014). Rapid magma evolution constrained by zircon petrochronology and 40Ar/39Ar sanidine ages for the Huckleberry Ridge Tuff, Yellowstone, USA. *Geology*, *42*(8), 643–646.

Rivera, T. A., Storey, M., Schmitz, M. D., & Crowley, J. L. (2013). Age intercalibration of ^{40}Ar/^{39}Ar sanidine and chemically distinct U/Pb zircon populations from the Alder Creek Rhyolite Quaternary geochronology standard. *Chemical Geology*, *345*, 87–98.

Roche, O., & Druitt, T. H. (2001). Onset of caldera collapse during ignimbrite eruptions. *Earth and Planetary Science Letters*, *191*(3), 191–202.

Rojas-Ortega, E. (2016). *Litoestratigrafía, petrografía y geoquímica de la toba Llano, y su relación con el crater el Xalapazco, Caldera de Los Humeros, Puebla* (MS thesis, pp. 129). San Luis Potosí, México: IPICYT.

Saunders, K. E., Morgan, D. J., Baker, J. A., & Wysoczanski, R. J. (2010). Themagmatic evolution of theWhakamaru Supereruption, New Zealand, constrained by a microanalytical study of plagioclase and quartz. *Journal of Petrology*, *51*(12), 2465–2488.

Scandone, R. (1990). Chaotic collapse of calderas. *Journal of Volcanology and Geothermal Research*, *42*(3), 285–302.

Schmitt, A. K. (2011). Uranium series accessory crystal dating of magmatic processes. *Annual Review of Earth and Planetary Sciences*, *39*(1), 321–349.

Smith, R. L. (1979). Ash-flow magmatism: Ash-flow tuffs. *Geological Society of America Special Paper*, *180*, 5–27.

Smith, R. L., & Shaw, H. R. (1975). Igneous-related geothermal systems. *U.S. Geological Survey Circular*, *726*, 58–83.

Smith, R. L., & Shaw, H. R. (1979). Igneous-related geothermal systems. *U.S. Geological Survey Circular*, *790*, 12–17.

Solari, L. A., Gomez-Tuena, A., Bernal, J. P., Perez-Arvizu, O., & Tanner, M. (2010). U-Pb zircon geochronology with an integrated LA-ICP-MS microanalytical workstation: Achievements in precision and accuracy. *Geostandards and Geoanalytical Research*, *34*(1), 5–18.

Solari, L. A., Ortega-Obregón, C., & Bernal, J. P. (2015). U–Pb zircon geochronology by LAICPMS combined with thermal annealing: Achievements in precision and accuracy on dating standard and unknown samples. *Chemical Geology*, *414*, 109–123.

Verma, S. P., Gómez-Arias, E., & Andaverde, J. (2011). Thermal sensitivity analysis of emplacement of the magma chamber in Los Humeros caldera, Puebla, Mexico. *Search Results International Geology Review*, *53*(8), 905–925.

Wark, D. A., Hildreth, W., Spear, F. S., Cherniak, D. J., & Watson, E. B. (2007). Pre-eruption recharge of the Bishop magma system. *Geology*, *35*(3), 235–238.

Wiedenbeck, M., Hanchar, J. M., Peck, W. H., Sylvester, P., Valley, J., Whitehouse, M., . . . Zheng, Y. F. (2004). Further Characterisation of the 91500 Zircon Crystal. *Geostandards and Geoanalytical Research*, *28*(1), 9–39.

Willcox, C. P. (2011). *Eruptive, magmatic and structural evolution of a large explosive caldera volcano: Los Humeros, Central México* (PhD thesis, 321 p.). Leicester, UK: University of Leicester.

Wilson, C. J. N., Gravley, D. M., Leonard, G. S., & Rowland, J. V. (2009). Volcanism in the central Taupo Volcanic Zone, New Zealand: Tempo, styles and controls. In *Studies in volcanology: The legacy of George Walker, Special publications of IAVCEI* (Vol. 2, pp. 225–247). London: The Geological Society.

Wohletz, K., Civetta, L., & Orsi, G. (1999). Thermal evolution of the Phlegraean magFor submissionmatic system. *Journal of Volcanology and Geothermal Research*, *91*(2), 381–414.

Wotzlaw, J.-F., Bindeman, I. N., Stern, R. A., D'abzac, F.-X., & Schaltegger, U. (2015). Rapid heterogeneous assembly of multiple magma reservoirs prior to Yellowstone supereruptions. *Scientific Report*, *5*(1), 14026.

Wotzlaw, J. R.-F., Bindeman, I. N., Watts, K. E., Schmitt, A. K., Caricchi, L., & Schaltegger, U. (2014). Linking rapid magma reservoir assembly and eruption trigger mechanisms at evolved Yellowstone type supervolcanoes. *Geology*, *42*(9), 807–810.

Wotzlaw, J. R.-F., Schaltegger, U., Frick, D. A., Dungan, M. A., Gerdes, A., & Günther, D. (2013). Tracking the evolution of large-volume silicic magma reservoirs from assembly to supereruption. *Geology*, *41*(8), 867–870.

Yáñez, C., & García, S. (1982). *Exploración de la región geotérmica Los Humeros-Las Derrumbadas, Estados de Puebla y Veracruz* (Internal report, pp. 1–96). Mexico City: Comisión Federal de Electricidad.